Journal of Thermal Analysis and Calorimetry, Vol. 93 (2008) 1, 7–17

THERMAL PROPERTIES OF ALIPHATIC NYLONS AND THEIR LINK TO CRYSTAL STRUCTURE AND MOLECULAR MOTION

B. Wunderlich[*]

Department of Chemistry, The University of Tennessee, Knoxville, TN 37996-1600, USA

The phase behavior of semicrystalline, aliphatic nylons is analyzed on the basis of differential scanning calorimetry, DSC, and quasi-isothermal, temperature-modulated DSC, TMDSC. The data of main interest are the apparent heat capacities, C_p, in the temperature range from below the glass transitions to above the isotropization. Based on the contributions of the vibrational motion to C_p, as is available from measurements in our laboratory, the ATHAS Data Bank, and multifaceted new TMDSC results, as well as on information on the crystal structures, NMR, molecular dynamics simulation of paraffin crystals, and quasi-elastic neutron scattering, the following observations are made: (a) In semicrystalline nylons the glass transition of the mobile-amorphous phase is broadened to higher temperature. The additionally present rigid-amorphous phase, RAF, undergoes a separate, broad glass transition at somewhat higher temperature. (b) The transition of the RAF, in turn, overlaps usually with an increase in large-amplitude motion of the CH_2-groups within the crystals and latent heat effects due to melting, recrystallization, and crystal annealing. (c) Above the glass transitions of the two non-crystalline phases, C_p of the crystals approaches and exceeds that of the melt. This effect is due to additional entropy contributions (disordering) within the crystals, which may for some nylons lead to a mesophase. In case a mesophase is formed, the C_p drops to the level of the melt as is common for mesophases. (d) Some locally reversible melting is present on the crystal surfaces, but seems to be minimal for the mesophase. (e) The increasing amount of large-amplitude motion in the crystals is described as a third glass transition, occurring over a broad temperature range below the melting or disordering transition from crystal to mesophase.

The assumption of a separate glass transition in ordered phases was previously discovered on analyzing aliphatic poly(oxide)s such as poly(oxyethylene), POE, and in the broad class of mesophase-forming small and large molecules. To attain a full description of the globally-metastable, semicrystalline phase-structure of nylons and to understand its properties, one needs quantitative information about the glass transitions of the two non-crystalline phases and that of the crystal, as well as the various irreversible and locally reversible order/disorder transitions and their kinetics. Finally, with different substitutions in the α-position of the backbone structure of nylon 2, one describes poly(amino acid)s which on proper copolymerization yield proteins. This links the present study to the earlier thermal analyses of all naturally occurring poly(amino acid)s, a number of copoly(amino acid)s, and globular proteins in their dehydrated states. It will be of importance to check by quantitative thermal analysis if similar glass transitions and phase structures as seen in the aliphatic nylons are also present in the poly(amino acid)s to possibly gain new information about the nanophase structure of proteins.

Keywords: *crystal structure, glass transition, heat capacity, isotropization, melting, mesophase, molecular motion, nylon, phase behavior, poly(amino acid), protein*

Introduction

The aliphatic nylons, or polyamides, form a homologous series of synthetic polymers. Nylon 6, for example, has the repeating unit [NH–CO–(CH_2–)$_5$] with the structure-based name poly[imino(1-oxohexamethylene)], i.e., it has six carbon backbone atoms in the repeating unit. Nylon 6.6, a structural isomer of nylon 6 with double the number of imino and carbon backbone atoms in the repeating unit is represented by [NH–CO–(CH_2)$_4$–CO–NH–(CH_2)$_6$–] and called poly(iminoadipoylhexamethylene), based on the structure of the adipic acid with six carbon atoms. The nylons find extensive applications in textiles, carpets, brushes and in bulk as engineering plastics [1]. Nylon 6.6 was first synthesized and analyzed in the laboratories of DuPont de Nemours and Co. [2]. The first fibers were introduced commercially in 1938 under the trade name 'Nylon', which by now is the generic term for the polyamides. In this paper, the thermal properties of the nylons gained by standard differential scanning thermal analysis, DSC, and the more modern temperature-modulated DSC, TMDSC, are discussed as they relate to molecular motion and their microphase and/or nanophase structure. Combining DSC and TMDSC allows not only to measure changes in total heat content or enthalpy, dH, with temperature, T, and composition, n, at constant pressure, p, as given by:

$$dH = (\partial H/\partial T)_{p,n}\, dT + (\partial H/\partial n)_{p,T} dn \qquad (1)$$

but also the separation of the two contributions. The first represents the heat capacity, $C_p[=(\partial H/\partial T)_{p,n}]$, and the second, the latent heat, $L[=(\partial H/\partial n)_{p,T}]$. In a standard DSC experiment, only an apparent heat capacity $C_p^{\#}(=dH/dT)$ can be quantitatively evaluated. It con-

* Wunderlich@CharterTN.net

1388–6150/$20.00

Akadémiai Kiadó, Budapest, Hungary
Springer, Dordrecht, The Netherlands

sists of both contributions to Eq. (1), with the second depending on dn/dT, the amount of phase transformations with latent heats during the change of temperature. This second part can be assessed by TMDSC with proper choice of frequency and heating or cooling rate since it can be written as $(dn/dt)/(dT/dt)$ which introduces the time, t, with the ratio of the rate of transformation and the rate of temperature change [3]. It will be shown, that in order to account for the results, semicrystalline nylons must be described as one-component, three-phase systems containing crystals and two noncrystalline phases with different glass transitions. Based on the phase rule, thermodynamic reasoning suggests that such a system cannot be stable. If it is metastable at low temperatures, it must have been arrested. For example, on cooling from the melt it does not reach the equilibrium represented by full crystallization. Furthermore, liquid-like motion observed in the crystals [4–8] will be interpreted as a glass transition without change in crystal structure. Depending on the type of nylon, the Brill transition [9] to a mesophase with a more symmetric crystal structure may occur above this glass transition. Only if all these aspects are considered, is it possible to fully understand the structure-property-processing triangle. Finally, it will be suggested that the proteins may show a similar phase structures as the nylons, since they are complex copolymers of differently substituted nylon 2 repeating units.

It is a pleasure to contribute this paper to the session honoring Dr. Howard Starkweather who, with his colleagues at DuPont, has contributed so much to our basic understanding of the nylon 6.6 X-ray diffraction, phase structure, transitions, and properties [1, 10–18], as well as the molecular motion, as measured by NMR [5–7]. An example of the importance of this work is shown in Fig. 1a. It is one piece of evidence that now, about 25 years later, provides support for the suggestion of a glass transition of the crystalline nylons. Figure 1a shows the temperature-dependence of the density of nylon 6.6 crystals as measured by X-ray diffraction [12]. The curve and analysis were added recently [19] and will be described in this paper. From Fig. 1a the glass transition temperature, T_g, can be surmised to be at ≈409 K the temperature where the expansivity has increased to a level similar to that of the melt. The subsequent decrease in expansivity at ≈455 K is caused by the phase transition of the triclinic crystals to the pseudo-hexagonal mesophase (condis crystal), which then change at T_m to the isotropic melt (≈525 K), which should for nylon 6.6 properly be called the isotropization temperature of the condis crystals, T_i. The equilibrium melting temperature is usually given at the much higher temperature, T_m^o≈574 K [20–22].

The left graph in Fig. 1b illustrates the time-dependence of melting in nylon 6. The behavior with increasing heating rate changes from superheating for the zone-polymerized and to some degree also for the melt-annealed sample, to a decreasing melting temperature due to less perfection of the initial crystals [23]. The right diagram is a comparison of the multiple endotherms of samples crystallized at different temperatures [24]. The amount of the two common polymorphs of the nylon 6 crystals are given by the bar graph on top. For the heating rate used, the horizontal lines 1 and 2 illustrate the limit of crystal perfection relative to the corresponding, less perfected crystals in 4 and 3. Line 5 shows what has been termed an annealing peak [25] which goes parallel to the indicated hypothetical equilibrium line where T_m=T_c. In Fig. 1c, the big differences in melting characteristics in drawn nylon 6 are described for crystals prevented from reorganizing by chemical cross-linking in the amorphous phase, [method C) [26]]. Method A) falsely shows hardly any effect on drawing, method B) illustrates only the superheating on fusion when the randomization of the melting molecules is hindered by remaining orientation in the amorphous parts. Only method C) allows an analysis of the initial crystals produced at different draw ratios and temperatures [graph D)]. Figures 1b and c, thus, illustrate the changes which can arise in crystals during measurement. In this paper, the complex behavior of nylons will be discussed which is commonly missed by qualitative, standard DSC where only uncalibrated heat-flow rates with endotherms and exotherms are recorded. The thermal properties of the nylons are shown to be complicated by rigid-morphous phases, RAF, [27] and glass transitions in crystals, both of which have strong effects on the mechanism of drawing of fibers. With hindsight, it is obvious from the graph D) in Fig. 1c that the nylon 6 crystals drawn at 443 K, above T_g of the crystals, should be, and are, most perfected. Drawing the semicrystalline fiber at 393 K, above the glass transition of the surrounding RAF, has a much smaller effect, and drawing at 328 K, in the vicinity of T_g of the mobile-amorphous phase, shows the least effect on perfection of the initial crystals.

Figure 1d depicts the first observation of a glass transition in crystals. Poly(oxyethylene), POE has a T_g which is 17 K below the melting temperature, T_m [28]. The shaded area clearly illustrates that the crystals reach the heat capacity (and molecular mobility) of the liquid before significant melting. At 339 K, at the reversing melting peak of the sample with molar mass 900,000 Da, POE900k, the total remaining crystallinity is still 55% when measured after long-time modulation [29]. Measurements by X-ray diffraction of POE crystals shows no evidence of a mesophase before melting [28].

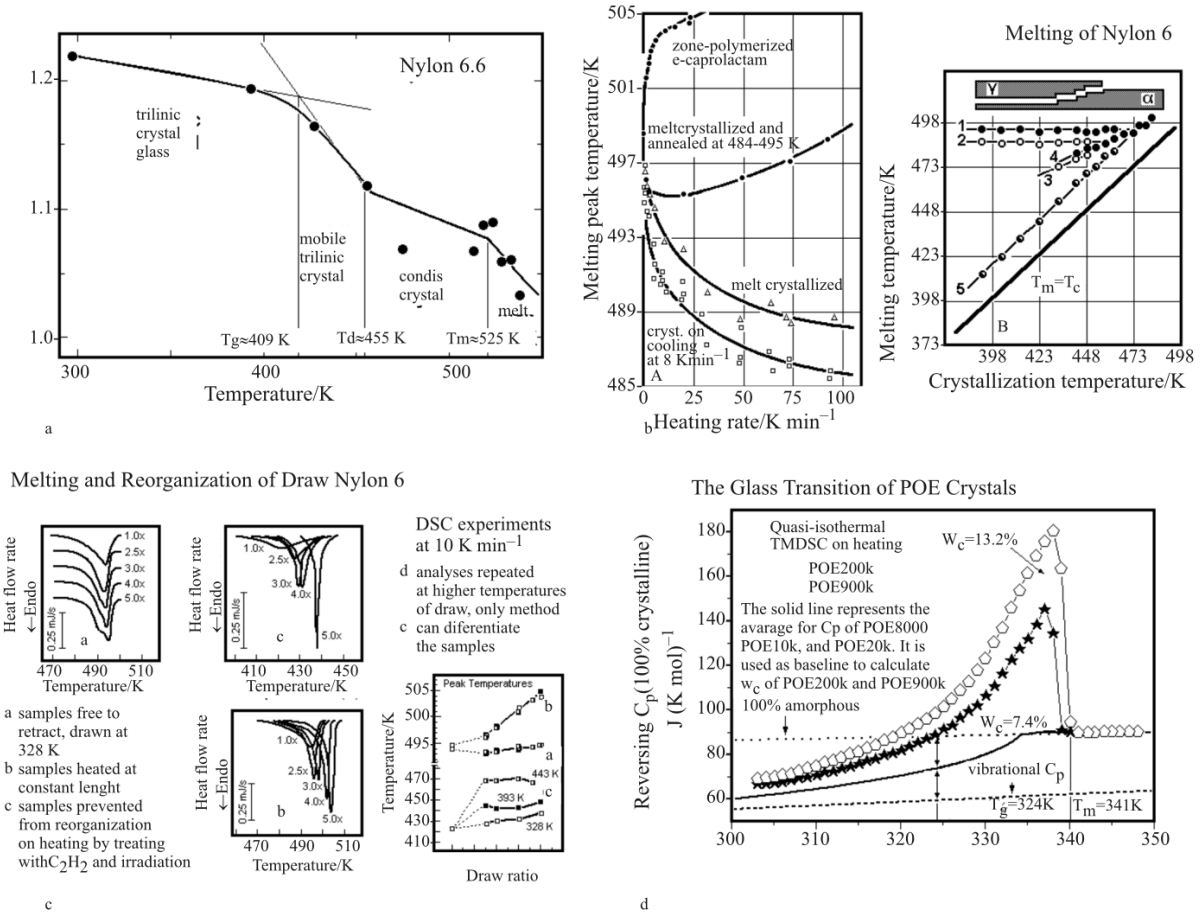

Fig. 1 a – Crystalline density of nylon 6.6 by temperature-resolved X-ray diffraction [12]. b – (left) Changes of the melting temperature of nylon 6 by DSC as a function of heating rate [23]. b – (right) Multiple melting peak temperatures of melt-crystallized nylon 6 by DSC at 8.0 K min^{-1} [24]. c – Changes of DSC traces of variously drawn nylon 6 fibers at different temperatures when changing the analysis method [26]. Only method C) permits conclusions about the initially present crystals. d – The glass transition of high molar mass crystals of poly(oxyethylene), POE. The crystallinity, w_c, by standard DSC, is 70%. Perfect, low-molar-mass crystals have no reversing melting peak, w_c >90%, and still show the T_g illustrated [28]

Experimental heat capacities and phase transitions

After introducing the manyfold transition behavior of nylons, it is now important to analyze the C_p of solids, to subtract the first term on the right of Eq. (1) from the measured dH in order to study the second term, i.e., evaluate the latent heat effects. The $C_p^{\#}$ of different semicrystalline nylons was measured [30] and compared to the literature [31]. Figure 2a illustrates a recent standard DSC trace of a semicrystalline nylon 6.6 over the temperature range of interest [19, 31], and Fig. 2b shows that C_p of all homologous liquid nylons can be represented by a single equation [30]. The question to be answered in this Section concerns the reasons and limits of the additivity of C_p with chemical structure.

At temperatures below 320 K, C_p of the nylon 6.6 crystals in Fig. 2a is fully described by the contributions from vibrations [32] and was critically evaluated using the ATHAS Data Bank [31]. The C_p of the noncrystalline glass of nylon 6.6 can be described from ≈50 K up to T_g(=323 K) by the same vibrational spectrum [30]. Above T_g or the isotropization temperature, T_i, the C_p of liquid nylon 6.6 matches the equation in Fig. 2b. Between 323 and 550 K, however, one needs a combination of DSC and TMDSC to separate the two contributions to the apparent $C_p^{\#}$ derived from Eq. (1). The molecular motion which produces the energetics of C_p is seen best in a molecular-dynamics simulation of the sequences of CH_2 groups in polyethylene by supercomputer, as drawn in Figs 2c and d [33].

From the experience gathered by comparing C_ps of more than 200 linear, flexible macromolecules, listed in the ATHAS Data Bank [31], it was found that the C_p of solids is easily described by an approximate frequency spectrum. While the C_p of simple metals are often represented by a single Debye function [34], flexible linear macromolecules need a combination of two, a one- and a three-dimensional Debye function, as was first suggested by Tarasov [35]. The three-di-

mensional Debye function is representative of intermolecular vibrations of the chains and has a typical Θ_3-temperature between 40 and 200 K, while the one-dimensional Debye function represents the intramolecular chain vibrations with a typical Θ_1 between 100 and 1000 K. The values of Θ (=$h\nu/k$, where h and k are Planck's and Botzmann's constant, respectively) are fixed by the upper frequency levels and indicate the temperature where the corresponding contributions to C_p reaches 92% of the Dulong–Petit level (R≈8.3 J K^{-1} mol^{-1}). Within homologous series, Θ varies little except for the first members. The additional group vibrations arise from strongly-bound atomic clusters which vibrate almost independently of the backbone skeleton and are largely localized, in contrast to the coupled skeletal vibrations [36]. The skeletal vibrations can be recognized in Fig. 2c by comparing the crystal at 0 K to the two snapshots at different times after heating to 80 K. To simplify the simulation, the group vibrations were eliminated in Figs 2c and d by using a unified-atom model.

The Θ-temperatures of the nylons and poly(amino acid)s as a homologous series vary only little with structure. For the common crystallinities of the nylons one finds a Θ_3 from 65–84 K, and a Θ_1 from 420–907 K, compared to the respective values of 80 and 519 for amorphous and 158 and 519 K for fully crystalline polyethylene. Adding the skeletal vibrations to the group vibrations, which are known precisely from IR and Raman spectra and are similar for the same atomic groupings in different molecules, one can understand the approximate additivity of C_p in the solid state. The liquid C_p, finally, can be explained with help of the large-amplitude conformational motion of the chains, exemplified by the time-sequence in Fig. 2d which also

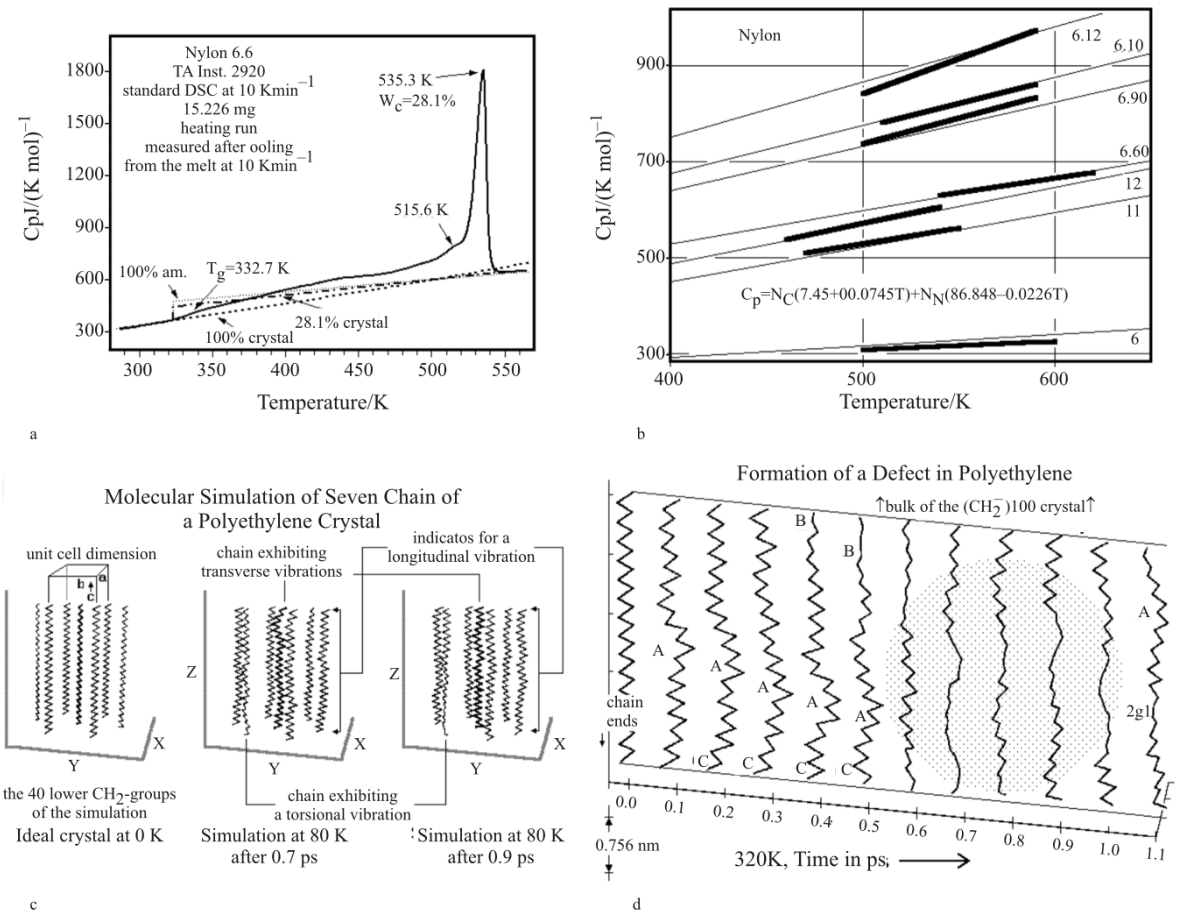

Fig. 2 a – Apparent heat capacity of melt-crystallized, dry nylon 6.6, measured by standard DSC and compared to the crystalline and (or glassy), liquid and semicrystalline values [19, 31]. b – Heat capacity of liquid nylons. The heavy lines mark the experimental data and the thin lines, the values of the equation. The number of backbone carbon and nitrogen atoms are represented by N_C and N_N [30]. c – Supercomputer simulation of a sequence of CH_2-groups in polyethylene, after heating to the indicated conditions [33], as they are also found in the nylon crystals. d – A single chain segment as in c – after different times of simulation, illustrating the collision of transverse (A), torsional (B) and longitudinal (C) phonons to form a defect of two gauche conformations separated by a single trans conformation, 2g1 [33]. This is an example of a large-amplitude conformational motion. Note the twist introduced into the chain

Table 1 Values of N_s, Θ_1, Θ_3, errors in C_p and temperature ranges of measurement

Biopolymer	N_s	Θ_1/K	Θ_3/K	% av and rms	T/K
polyalanine	9	634	58	–0.5±1.3	60–390
polyglycine	6	750	91	–1.5±5.2	1.4–390
polyvaline	14	664	65	0.7±2.6	2–390
polymethionine	15	542	83	–0.5±1.6	5–200
polyphenylalanine	11	396	67	1.4±3.5	5–300
insulin	628	599	79	0.01±3.1	10–310
chymotrypsinogen	3005	631	79	0.5±3.2	10–310
ribonuclease A	1574	717	(79)	–0.69±2.2	130–420
lactoglobulin	2188	586	91	–0.47±4.5	7–200
ovalbumin	5008	637	83	–1.06±4.8	5–200
lysozyme	1665	618	79	0.42±5.1	7–200

gives the picosecond time scale of the motion involving defect generation.

Figures 3a and b show an application of this analysis of C_p in terms of the molecular motion in the solid state to the protein bovine Θ-chymotryp- sinogen, a molecule of 245 amino acids distributed over all 20 naturally-occurring amino acids. Its molar mass is 25,646 Da. All contributions to C_p by the group vibrations were calculated from data on the pure poly(amino acid)s [37, 38] and subtracted from the total C_p, as seen from Fig. 3b. Next, the contributions of the 3005 skeletal vibrations, N_s, were fitted as is illustrated in Fig. 3a. A 20×20 mesh with Θ_3 values between 10 and 200 K and Θ_1 values between 200 and 900 K was calculated point by point and then fitted by a least square method to the experimental C_p with the result shown in Fig. 3a [39]. It is seen that a unique minimum exists in this analysis, as was found before for the simpler synthetic polymers. The Table, below, shows results for five poly(amino acid)s and six proteins [40]. Note the small variation in Θ and the good fit to the experimental C_p illustrated in Fig. 3b. Once the C_p of the solid is available, it can be extrapolated safely into the phase-transition region and combined with the empirically obtained C_p of the liquid for an analysis as is indicated in Fig. 2a.

Before adding TMDSC data to the discussion of apparent C_p, the phase transitions are summarized with Figs 3c and d. The traditional assumption is that the mobile states of mesophases and liquids are reached either by a glass, disordering, or melting transition. It was earlier suggested [41] that all solid states become mobile at a glass transition temperature, T_g, with T_g being identified by the change of C_p from that of a vibrator to that of a mobile state with cooperative, large-amplitude motion [41, 42]. This suggestion is supported by the observation that all glasses have similar viscosities at T_g ($\approx 10^{12}$ Pa s), i.e., they have a similar resistance to deformation as a measure of solidity, while crystal properties vary widely. For crystals which are 'solid' at the melting temperature the loss in order and the glass transition occurs at the same temperature, as indicated in Fig. 3c. For the POE in Fig. 1d and aliphatic nylon crystals, however, could be shown that the glass transition occurs before melting, and in nylon 6.6, it even occurs before the transition to the mesophase, as indicated in Fig. 3d [19]. In general, it is expected that the larger the order, the tighter is the packing of the molecules, causing a higher T_g, ultimately moving it to the disordering or melting transition (T_d or T_m, respectively) as shown in Fig. 3c.

TMDSC results between glass transition and isotropization

An important tool to evaluate the apparent $C_p^{\#}$ of semicrystalline polymers is the quasi-isothermal TMDSC [43]. In quasi-isothermal TMDSC many isotherms are run in sequence of increasing or decreasing temperature. To these isotherms, a small modulation of the sample temperature is added with an amplitude, usually between 0.1 and 3.0 K and a frequency between 0.1 and 0.0025 Hz. Figures 1d and 4a to c show the C_p calculated from the response of the samples to such modulations [19, 28]. A direct analysis of such data yields a 'reversing' C_p. The thermodynamic C_p, as seen in Figs 2c and d, is based on vibrations and large-amplitude conformational motions which have time scales of picoseconds (10^{-12} s). This is so fast, that the sample response to the modulation is limited only by the time scale of the calorimeter, set by its construction, the involved thermal conductivities, and the size of the samples. Outside the transition ranges, once calibrated, TMDSC and DSC should measure the same, reversible, thermodynamic C_p. In these temperature ranges only the first term on the right side of Eq. (1)

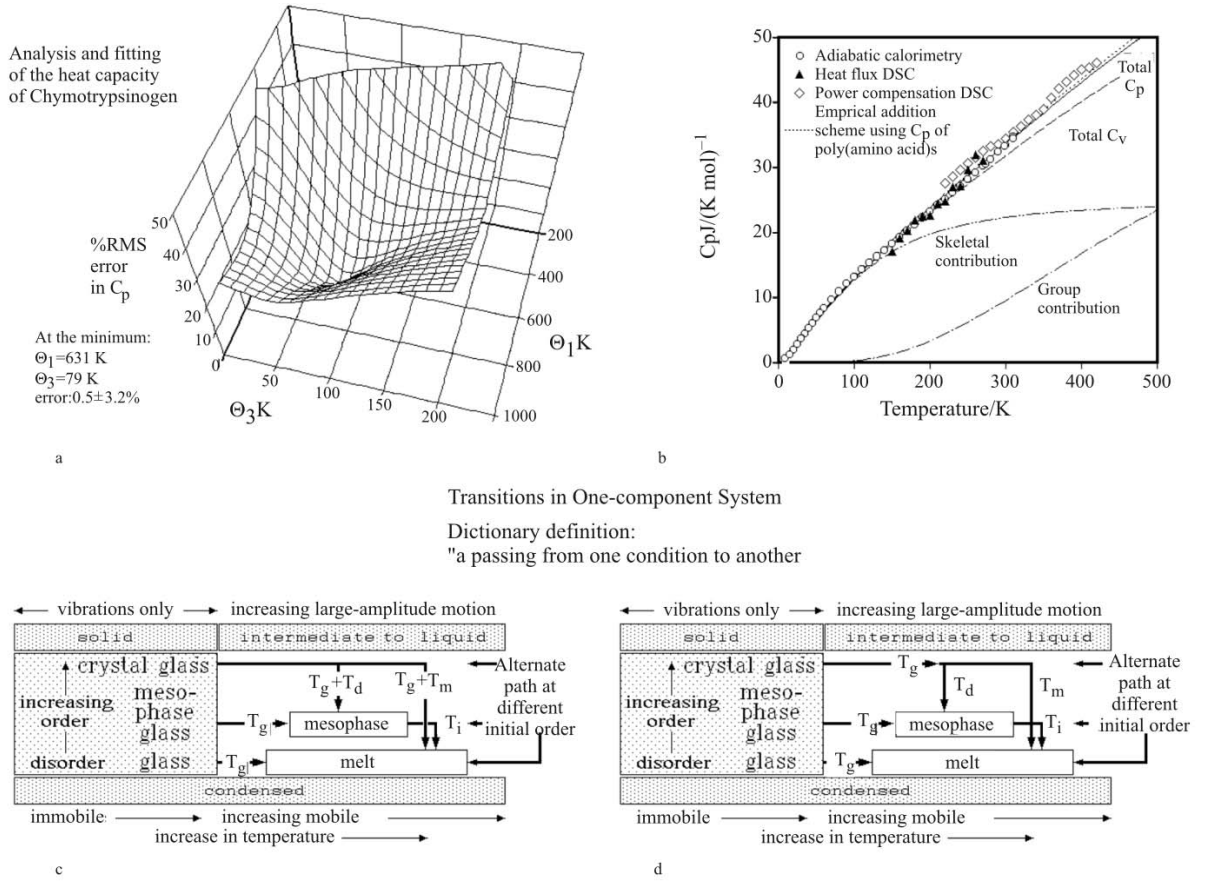

Fig. 3 a – Proof of the unique fit of the skeletal vibrations to a combination of one- and two-dimensional Debye functions. b – Combination of the heat capacities from the skeletal and group vibration to C_v and C_p and comparison to heat capacities measured with different calorimeters [39]. c – Schematic of the transitions of an amorphous glass, a mesophase glass, and a crystal to the melt (liquid) with the assumption that disordering and melting (isotropization) occur at the same temperature. d – Expanded schematic which allows for the here suggested possibility of separate glass and disordering transitions in nylon 6.6

contributes to dH. Within the transition regions, latent heat terms or slow cooperative large-amplitude motions may give much slower contributions to dH and can be separated from the fast response. Particularly the latent-heat response due to melting, crystallization, annealing, and reorganization may be sufficiently slow to be analyzed by the special methods of analysis to be shown in this Section.

The standard duration of the modulation in our quasi-isothermal TMDSC is 20 min, with the data from the last 10 min being averaged for analysis. If after 10 min the response to the modulation is constant, this is taken as an indication that the measurement is reversible. The reversible data are in contrast to the 'reversing data' which are not checked for reversibility and may change slowly with modulation time and then have different, asymmetric heating and cooling responses. Changing order within a sample is a common cause of changing reversing C_p with time. If such behavior was suspected or seen directly, separate long-time modulation experiments were performed for 600 min. By fitting a series of 10 min long evaluations to exponential functions, these experiments were then extrapolated to infinite time to estimate a reversible heat capacity. Although it is obvious from Fig. 4a that most of the melting peak is irreversible, there seems some reversibility left, as has been also observed for many other semicrystalline linear macromolecules. It was suggested that this is a locally reversible melting of the overall metastable structure at the growth face of the crystals [44]. Equilibrium crystals with an extended-chain macroconformation and also sharply folded, close to perfect crystals seem to show no reversible melting [28], while the reversible melting increases with imperfection [44], as can also be deduced from Fig. 1d, where the higher molar mass with the higher reversible melting has the poorer crystals and lower crystallinity [28]. Comparing the total C_p by DSC of nylon 6.6 to the other nylons (6, 11, 12, 6.9, 6.10, and 6.12), one finds that all exceed the expected C_p calculated for the given crystallinity [30]. This observation was analyzed, as much as pos-

sible, based on the two assumptions, a second amorphous phase of higher T_g surrounding the crystals, an RAF, and possible mobility within the crystalline fraction [45[. A liquid-like molecular motion in the crystals was supported by quasi-elastic neutron scattering [8], NMR [4–7], and X-ray analyses [12, 45]. In this paper, it is interpreted as a glass transition without change in crystal structure, as illustrated schematically in Fig. 3d. A full transformation to a mesophase may or may not occur in any given nylon.

Figure 4a is a comparison of the apparent C_p of two initially identical samples of nylon 6.6 by standard DSC on heating, shown also in Fig. 2a, and by quasi-isothermal TMDSC at the indicated, increasing temperatures. This is followed in Fig. 4b with a sequence of quasi-isothermal TMDSC experiments starting at the melt with cooling in steps to below the lowest glass transition, followed by heating in similarly spaced steps back to the melt. Figure 4c reveals the effect of longer modulation time on a sample similar to the one in Fig. 4a, while Fig. 4d is a collection of standard DSC traces run at the end of the long-time modulations given in Fig. 4c.

The glass transition of amorphous nylon 6.6 occurs at 323 K [31]. On crystallization from the melt, this T_g changes to 332.7 K due to broadening of the transition to higher temperature, as is common in semicrystalline polymers [3]. In addition, there is evidence of 36% RAF since at the upper limit of the increase of C_p of the amorphous nylon 6.6 due to the glass transition is reached at 342 K, where C_p has reached less than 50% of the increase expected for a sample of 28% crystallinity (see the dash-dotted line in Fig. 2a). This crystallinity is estimated independently from the heat of fusion and agrees also with data from X-ray scattering. To find evidence for a separate T_g of the RAF, one can look at the reversing C_p in Figs 4a and b. There is no evidence of irreversible melting up to about 440 K (no change in reversing C_p with time is also noted in Fig. 4c), but a continuous increase in reversible C_p is seen which ultimately goes not only beyond that expected for the semicrystalline nylon 6.6, but also that of the liquid (at

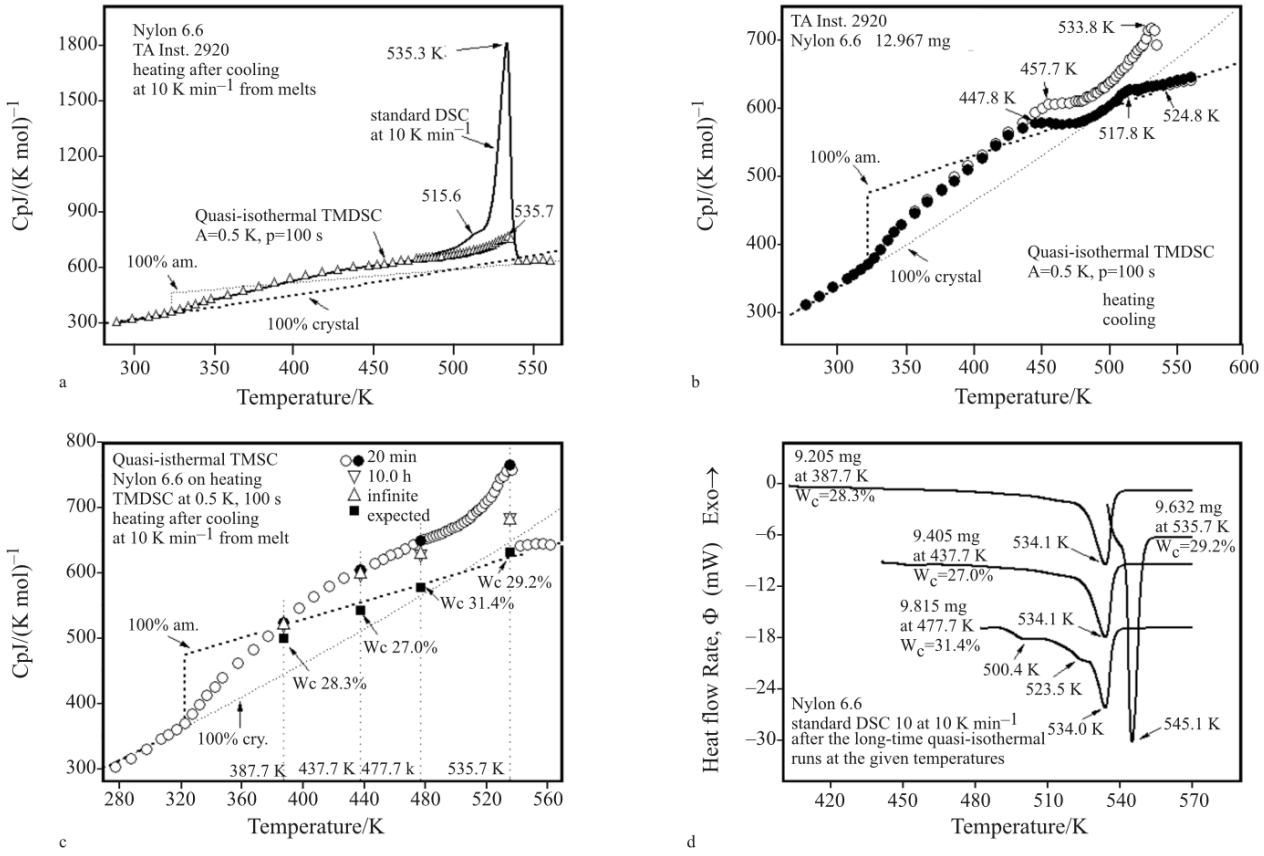

Fig. 4 a – Comparison of the standard DSC trace of Fig. 2a with quasi-isothermal TMDSC experiments [19]. b – Comparison of quasi-isothermal DSC experiments on cooling from the melt with subsequent heating. c – Repeat of the quasi-isothermal TMDSC experiments in Fig. 4a with long-time modulation at four selected temperatures. d – Analysis of the long-time modulated samples of Fig. 4c by subsequent standard DSC, illustrating the major crystal perfections occurring by long-time annealing

≈390 K). Similar results to those in Fig. 2a where also observed for the other, earlier studied nylons [30]. The increase to the level of the expected semicrystalline C_p makes it likely that the RAF in nylon 6.6 begins its glass transition somewhat above 342 K and is complete at perhaps ≈380 K, with a midpoint T_g estimated to be at 370 K. The crystal itself becomes mobile with an upper-end temperature of its glass transition at ≈440 K, which is also the approximate position of the Brill temperature, which was originally suggested to be at 435 K [9] and seems to be at 455 K in Fig. 1a [12].

A glass transition within the crystal [41], as mentioned in the Introduction, is now linked to the reversible C_p beyond the end of glass transition of the RAF at ≈380 K. At ≈440 K it reaches an excess C_p of about 60 J K^{-1} mol^{-1} beyond the semicrystalline level. The glass transition would be caused by the increase in segmental mobility of the methylene groups. The NMR studies prove such segmental motion [4–7]. Quasielastic neutron scattering studies showed, similarly, that at temperatures 40 K below melting, the CH_2-groups undergo liquid-like motion [8]. For nylon 6.6, the same is suggested by the gradual approach of the triclinic crystal structure to a hexagonal one [45] and its increase in volume. A hexagonal unit cell based on one chain, however, is not commensurate with the symmetry of the CH_2-groups [46], unless they average their position due to rotational motion caused by conformational disorder, as simulated in Fig. 2d. Similar observations were made on paraffins and polyethylene [47]. For all of these crystals an increase in C_p beyond the vibrational limit was observed, but not all paraffins as well as polyethylene reached a hexagonal mesophase (‘rotor phase’), although the beginning of this motion was seen in all. The introduction of defects as in Fig. 2d [33], thus, goes parallel with an increase in C_p. When interpreting this as the beginning of a glass transition of the crystal, it may go parallel with an increase in disorder of the crystal, which when completed may lead to a symmetric mesophase. Finally, the expansivity of the crystals, as gained from the time-resolved X-ray diffraction on the nylon 6.6 crystals in Fig. 1a, has similarly been analyzed as a glass transition at about 409 K. This temperature is in agreement with the increase in excess heat capacity, starting just after the glass transition of the RAF. To summarize, the sample analyzed in Fig. 4a has a glass transition of the mobile amorphous fraction at ≈333 K, a T_g of the RAF at ≈370 K, and a T_g of the crystal at ≈409 K.

The Brill transition of nylon 6.6 in Fig. 1a occurs at perhaps 455 K, somewhat higher than the glass transition. A recent review with close to 150 references [48] collects the many results which support that the same type of motion of the CH_2-sequences is involved in the glass transition of the crystal and a pre-isotropization Brill transition. At the transition point, recognized by equal external and internal X-ray diffraction peaks, the triclinic, low-temperature crystals have changed to the pseudo-hexagonal mesophase (condis crystal). The Brill temperature depends not only on structure (molecular and crystalline), but also on crystal perfection, deformation, and the possible presence of solvents. The glass transition, on the other hand, was shown on the example of POEs in Fig. 1d, not to require the average of the rotational motion about the chain axis to reach full symmetry. When looking at a diagram of the isotropization temperatures of the various nylons [49], one sees a change of as much as 200 K with CH_2-sequence length and it may reach below that of the disordering transition to the mesophase (which, in turn, is also dependent on the crystal structure) and then, naturally, precludes the Brill transition. Crystal perfection also influences the Brill temperature, as can be seen on the lower Brill temperature on cooling compared to heating [50]. The orientation influence was seen from the about 15 K higher Brill transition in the trans-crystallized portion of an otherwise spherulitic nylon 6.6 [51]. Finally, FTIR studies on an oligomer of nylon 6.6 with 100% crystallinity and an extended-chain macro-conformation has a Brill transition and no amorphous fraction. For such a sample no changes in the H-bond structure occur during the transition [51], as was also assumed above for the polyamide. For nylon 6.6 the glass temperatures and the Brill temperature are all far below the equilibrium melting temperature, estimated at 574 K [20–22].

The transitions in the other aliphatic nylons differ only in degree from nylon 6.6. The thermal analyses of nylon 6, 11, 12, 6.9, 6.10, and 6.12 were already considered above. All exceeded the expected C_p calculated for the given crystallinity [30], indicating the existence of large-amplitude motion within the cystal before isotropization. This motion was shown by X-ray diffraction and infrared analysis to lead to a Brill transition for nylon 2.16, 4.16, 6.10, 6.12, 6.16 and 10.10 [52–54]. More details were derived for nylon 10.10 [54–58]. Molecular dynamics calculations and thermal analysis data led to similar interpretations as displayed above for nylon 6.6. A glass transition of the crystals, however, was not proposed because of a lack of quantitative interpretation of the heat capacity.

The irreversible isotropization of nylon 6.6 starts at about 480 K, after the crystals have changed to the pseudo-hexagonal mesophase. It can be discerned from Fig. 4a, and its slow completion is obvious from Fig. 4c. Some details of melting, recrystallization, and

possible annealing during the long-time modulations can be surmised from Fig. 4d. Quasi-isothermal holding of the nylon 6.6 close to the reversing melting peak at 535.7 K clearly leads to a fully re-crystallized sample with the sharpest melting peak and a jump in peak temperature. Even the observed lower melting temperatures, however, are most likely increased by a large amount beyond their zero-entropy-production value by crystal perfection, as suggested by the experiments on fibers of nylon 6, reproduced in Fig. 1c (compare the data for the undrawn sample, draw ratio 1.0 in graph D) [26]. Similar changes are expected for nylon 6.6. The term 'zero-entropy-production melting' is taken from irreversible thermodynamics of melting [3]. It occurs at a temperature where the metastability of the initial crystal is equal to that of the supercooled melt.

At 535.7 K, the peak temperature of the reversing, apparent C_p of nylon 6.6 in Fig. 4c, more than half of the excess reversing contribution to C_p measured after 10 min of modulation is from slow, irreversible latent heats and has decayed after 600 min. This leads to the final question to be addressed: Is there any remaining reversible melting? Certainly, if the points Δ at 437.7 to 535.7 K in Fig. 4c are interpreted to be due to a constant excess heat capacity, there would be no significant reversible melting. Above the formation of the mesophase (Brill temperature, ≈455 K), however, there is no reason for a significant excess heat capacity beyond that of the melt because of the normal expansivity seen in Fig. 1a. The mesophase being fully symmetric, should have no further latent heat contribution, i.e., its C_p should be close to that of the melt. The analysis of the quasi-isothermal TMDSC on cooling, indeed, suggests in Fig. 4b (points •) that by 510 K, when the crystallization is largely completed [19] that the reversible heat capacity is close to that of the melt. From temperature-dependent X-ray diffraction data, taken on cooling from the melt, it was shown that the initially growing crystals are of the pseudo-hexagonal structure of the mesophase [22, 45, 50]. Figure 4b proves that the measured, reversible C_p settles to a level close to the C_p of the liquid after major crystallization is over, rather than the level measured on heating. At about 440 K, in the vicinity of the Brill temperature, where the triclinic crystal is observed, the reversible C_p increases to that measured on heating, and at lower temperatures is identical to the data on heating. This interpretation leaves room for the assignment of the difference between reversible C_p measured in Fig. 4b on heating and cooling to the reversible melting, similar to what is seen for many other polymer crystals [44].

Conclusions

In this paper, a large volume of thermal analysis data on nylons could be combined with direct analyses of large-amplitude molecular motion by molecular dynamics simulations of CH_2-groups in polymers, quasi-elastic neutron scattering, NMR, and X-ray diffraction to reach a more complete description of the phase structures and transitions. Typical semicrystalline, melt-crystallized linear macromolecules consist of a metastable microphase-structure with nanophase inclusions which are all coupled by the long-chain molecules which cross the phase boundaries (interfaces). In this picture, a microphase structure has dimensions of less than one micrometer, typical for the crystals of flexible macromolecules. Thermodynamically the microphase structures must always be described by adding information about their surface free energy to information about their bulk free enthalpy. Nanophase structures, in turn, are so small, that some or all of their bulk-properties are lost [59–63]. The thermodynamic C_p on various nylons were originally measured in our laboratory by standard DSC and combined with literature data and analyzed by Xenopoulos [22, 30, 32, 45]. This work was recently extended by Qiu for nylon 6.6 with extensive TMDSC measurements [19].

Based on these results, using the just summarized definitions, we conclude that the crystals of the nylons can be treated as microphases which, because of surface effects, have an isotropization temperature much lower than their equilibrium temperature. Rigid-amorphous nanophases (RAF) with a measurable glass transition temperature enclose these crystals. The identification of the RAF as a nanophase is made because it has no bulk glass transition which can be linked to the bulk-amorphous phase (which is often also called the mobile-amorphous fraction MAF). The lowest glass transition, largely separated from the T_g of the RAF, finally, reaches to the established T_g of the noncrystalline bulk samples and must be attributed to the remaining amorphous microphase. On heating, the crystals themselves develop large-amplitude motion, starting above the glass transition of the RAF. This gain in mobility is interpreted as a broad, third glass transition, well below the melting or isotropization temperature, and in the case of nylon 6.6 below the Brill transition to the pseudo-hexagonal condis phase. In this broad glass transition region of the crystals, a reversible latent heat of disordering is observed, causing an excess C_p. Finally, on the crystal surface, at temperatures within the irreversible melting peak there is a small fraction of decoupled chain segments which melts reversibly.

For the featured nylon 6.6 one, thus, finds below the low-temperature glass transition at 323 K a meta-

stable, rigid-amorphous microphase MAF which is connected via the RAF nanophases which, naturally, are also rigid, to the rigid triclinic microphase crystals (structure I). The glass transition of the MAF of about 36% of the analyzed sample is broadened and centers at 333 K. Above this temperature the phase structure consists of three well defined parts: 36% mobile-amorphous microphase (MAF), 36% rigid amorphous nanophase (RAF), and 28% microphase crystals (structure II). The next change is centered at 370 K, the separate glass transition of the RAF. Above this temperature the semicrystalline sample can be described as a two-phase structure. All 72% of the noncrystalline polymer is mobile (structure III). In a further step, the triclinic crystals start to undergo a glass transition with a midpoint at about 409 K and begin simultaneously to disorder in direction of a mobile mesophase (structure IV). At 435–455 K the mesophase transformation is complete, depending somewhat on sample type and history (structure V). The 28% pseudo-hexagonal condis crystals begin their irreversible isotropization at 480 K with a peak at 534–545 K and possibly some reversibly decoupled chain segments on their growth face (structure VI). Above this temperature, the nylon 6.6 is a single-phase mobile melt (structures VII) which above the equilibrium melting temperature of 574 K is finally an equilibrium phase (structure VIII). These eight distinguishable phase structures can undergo major changes in perfection in direction towards local and global equilibrium during heating, caused by annealing and recrystallization of the various micro- and nano-phases. For this complicated non-equilibrium structure, calorimetry is the key technique for its analysis, allowing proper assignment of equilibrium and nonequilibrium states with the help of DSC and TMDSC.

The mechnical properties of the nylons must next be linked to the eight-phase structures just outlined. It is obvious that the eight-phase structures differ widely. It should be difficult to draw structure I. Structure II would lead to major orientation in the mobile amorphous fraction and result in large shrinkage on heating though the glass transition. Drawing of structure III can additionally deform the RAF. When introducing partial orientation of these noncrystalline chain segments, they may order to some degree and release some latent heat, an observation made on fibers of gel-spun, ultrahigh molar mass polyethylene [64]. An orientation of the two amorphous phases is possible above the glass transition of the crystals, i.e., in structures IV and V, as was observed for gel-spun polyethylene [65]. Effects of this type became clear on reinspection of the literature data from Fig. 1c for the nylon 6 fibers. One would expect also differences in the morphology of the deformed crystals obtained in drawing depending on the ease of deformation of the surrounding, molecularly coupled, non-crystalline fractions. Much work remains to be done to properly link the thermodynamic phase structure of the nylons to their specific mechanical properties and may lead to a scientific base of many empirically obtained processing conditions.

Finally, one should look at possible future work that could lead to progress in the unending quest to better understand the structure-property-processing triangle with the use of thermal analysis. Many of the conclusions of this paper are based on the specific case of nylon 6.6, a more than 70-year-old industrial product, and details should be investigated also for the other polymers of this homologous series, as well as for other polymers. Most intriguing, however, is the possibility to expand the work into the substituted nylon-2 polymers, the proteins, and other biopolymers of different molecular composition, such as the carbohydrates. As pointed out in the discussion of Figs 3a and b, all naturally occurring polyamino acids have been analyzed [37–40] and several copolymers and proteins have similarly been studied with respect to their heat capacity. Similarly, carbohydrates have seen some attention in the form of amorphous starch and starch and water systems [66, 67]. In these cases an analysis of the detailed phase structure could reveal new aspects of the functioning of these more complicated systems by identifying their nanophase structure.

Overall, this paper and others like it, have shown that quantitative DSC coupled with TMDSC can open new information on the phase structure. One should always remember that most modern DSC equipment in use today is fully capable to yield not only qualitative DSC curves of un-calibrated heat-flow rates *vs.* time or temperature, but also high precision, apparent heat capacities which can be interpreted as in the case of the nylons when based on Eq. (1).

References

1 M. I. Kohan (Ed.), Nylon Plastics Handbook, Hanser Gardener: Cincinnati, 1995; see in particular: Chapter 5 on Physical Structure by A. Xenopoulos and E. Clark, pp. 107–138 and Chapter 6 on Transitions and Relaxations by H. W. Starkweather, Jr.,139–150.
2 H. Mark and G. E. Whitby, Collected Papers of Wallace H. Carothers on Polymerization. Interscience, New York 1940.
3 B. Wunderlich, Thermal Analysis of Polymeric Materials, Springer-Verlag, Berlin 2005.
4 W. P. Slichter, J. Polym. Sci., 35 (1958) 77.
5 J. Hirschinger, H. Miura, K. H. Gardner and A. D. English, Macromolecules, 23 (1990) 2153.
6 H. Miura, J. Hirschinger and A. D. English, Macromolecules, 23 (1990) 2169.

7 J. Wendoloski, K. H. Gardner, J. Hirschinger, H. Miura and A. D. English, Science, 247 (1990) 431.
8 A. Xenopoulos, B. Wunderlich and A. H. Narten, Macromolecules, 26 (1993) 1576.
9 R. Brill, J. Prakt. Chem., 161 (1942) 49.
10 D. Garcia and H. W. Starkweather, Jr., J. Polym. Sci., Polym. Phys. Ed., 23 (1985) 537.
11 H. W. Starkweather, Jr., P. Zoller, G. A. Jones and A. Glover, J. Polym. Sci., Polym. Phys. Ed., 22 (1984) 1615.
12 H. W. Starkweather, Jr., G. A. Jones and A. Glover, J. Polym. Sci., Polym. Phys. Ed., 19 (1981) 467.
13 H. W. Starkweather, Jr. and J. R. Barkley, Polym. Phys. Ed., 19 (1981) 1211.
14 H. W. Starkweather, Jr., J. F. Whitney and D. R. Johnson, J. Polym. Sci., Pt. A, 1 (1963) 715.
15 H. W. Starkweather, Jr. and R. E. Moynihan, J. Polym. Sci., 22 (1956) 363.
16 H. W. Starkweather, Jr., G. E. Moore, J. E. Hansen, T. M. Roder and R. E. Brooks, J. Polym. Sci., 21 (1956) 1892.
17 H. W. Starkweather, Jr. and R. E. Brooks, J. Appl. Polym. Sci., 1 (1959) 236.
18 H. W. Starkweather, Jr., J. Appl. Polym. Sci., 2 (1959) 129.
19 W. Qiu, A. Habenschuss and B. Wunderlich, Polymer, 48 (2007) 1641.
20 H. Haberkorn, K.-H. Illers and O. Simak, Colloid Polym. Sci., 257 (1979) 820.
21 J. H. Magill, M. Girolamo and A. Keller, Polymer, 22 (1981) 43.
22 A. Xenopoulos, 'Thermal Analysis and Studies of Conformational Disorder in Aliphatic Polyamides.' Thesis, Rensselaer Polytechnic Institute, Chemistry, Troy, NY 1990.
23 F. N. Liberti and B. Wunderlich, J. Polym. Sci., Part A-2, 6 (1968) 833.
24 P. Weigel, A. Hirte and C. Ruscher, Faserforsch. Textiltechnik, 25 (1974) 129.
25 K. H. Illers, Prog. Colloid Polymer Sci., 58 (1975) 61.
26 M. Todoki and T. Kawaguchi, J. Polym. Sci., Polym. Phys. Ed., 15 (1977) 1068, 1507.
27 H. Suzuki, J. Grebowicz and B. Wunderlich, Br. Polym. J., 17 (1985) 1.
28 W. Qiu, M. Pyda, E. Nowak-Pyda, A. Habenschuss and B. Wunderlich, Macromolecules, 38 (2005) 8454.
29 W. Qiu and B. Wunderlich, Thermochim. Acta, 448 (2006) 136.
30 A. Xenopoulos and B. Wunderlich, J. Polym. Sci., Polym. Phys. Ed., 28 (1990) 2271.
31 U. Gaur, S.-F. Lau, B. B. Wunderlich and B. Wunderlich, J. Phys. Chem. Ref. Data, 12 (1983) 65. Extended by new measurements in [30]. See also, B. Wunderlich, 'The Athas Data Base on Heat Capacities of Polymers.' Pure Applied Chem., 67 (1995) 1019. For a collection of the updated critically analyzed data, see the ATHAS website: http://athas.prz.rzeszow.pl
32 A. Xenopoulos and B. Wunderlich, Polymer, 31 (1990) 1260.
33 B. G. Sumpter, D. W. Noid, G. L. Liang and B. Wunderlich, in U. Suter and L. Monnerie, Eds, Atomistic Modeling of Physical Properties of Polymers. pp. 27–72, Springer, Berlin 1994 (Adv. Polymer Sci., Vol. 116).
34 P. Debye, Ann. Phys., 37 (1912) 789.
35 V. V. Tarasov, Zh. Fiz. Khim., 24 (1950) 111.
36 B. Wunderlich and H. Baur, Heat Capacities of Linear High Polymers (transl. into Russian by Yu. Godovsky, Publishing House 'Mir', Moscow, 1972, p. 240.) Fortschr. Hochpolymeren Forsch. (Adv. Polymer Sci.), 7 (1970) 151.
37 K. A. Roles, A. Xenopoulos and B. Wunderlich, Biopolymers, 31 (1991) 477.
38 K. A. Roles and B. Wunderlich, Biopolymers, 33 (1993) 279.
39 G. Zhang, S. Gerdes and B. Wunderlich, Macromol. Chem. Phys., 197 (1996) 3791.
40 G. Zhang and B. Wunderlich, Proc. 25th NATAS Conf. in McLean, Va., Sept. 7–9, R. J. Morgan and R.G. Morgan, Eds, 25 (1997) 540.
41 B. Wunderlich, Thermochim. Acta, 446 (2006) 128.
42 B. Wunderlich, J. Appl. Polym. Sci., 105 (2007) 49.
43 M. Reading and D. J. Hourston, Eds, Modulated Temperature Differential Scanning Calorimetry, Springer, Dordrecht, The Netherlands 2006.
44 B. Wunderlich, Prog. Polym. Sci., 28 (2003) 383.
45 A. Xenopoulos and B. Wunderlich, Coll. Polym. Sci., 269 (1991) 375.
46 A. I. Kitaigorodskii, Organicheskaya Kristallokhimiya, Press of the Acad. Sci. USSR, Moscow 1955. Revised, English Translation by Consultants Bureau, New York 1961.
47 Y. Jin and B. Wunderlich, J. Phys. Chem., 95 (1991) 9000.
48 M. N. Sanjeeva, J. Polym. Sci., Part B: Polymer Phys., 44 (2006) 1763.
49 B. Wunderlich, Macromoleculer Physics, Vol. 3, Crystal Melting, Academic Press, New York 1980 (Section 10.3.2).
50 C. Ramesh, A. Keller and S. J. E. A. Eltink, Polymer, 35 (1994) 2483.
51 S. J. Cooper, M. Coogan, N. Everall and I. Priestnall, Polymer, 42 (2001) 10119.
52 W. Li, Y. Huang, G. Zhang and D. Yan, Polym. Int., 52 (2003) 1905.
53 H. J. Biangardi, J. Macromol. Sci., Phys., B29 (1990) 139.
54 Y. Yoshioka and T. Kohji, Polymer, 44 (2003) 6407.
55 T. Kohji, Chinese J. Polym. Sci., 25 (2007) 73.
56 Y. Yoshioka and T. Kohji, Polymer, 44 (2003) 7007.
57 Y. Yoshioka and T. Kohji, Polymer, 44 (2003) 6349.
58 T. Kohji and Y. Yoshioka, Polymer, 45 (2004) 4337.
59 B. Wunderlich, J. Thermal Anal., 49 (1997) 513.
60 W. Chen and B. Wunderlich, Macromol. Chem. Phys., 200 (1999) 283.
61 B. Wunderlich, Thermochim. Acta, 403 (2003) 1.
62 B. Wunderlich, Macromol. Rapid Commun., 26 (2005) 1521.
63 B. Wunderlich, Int. J. Thermophys. Fluid Phase Equilib., 89 (2007) 321.
64 J. Pak and B. Wunderlich, Thermochim. Acta, 421 (2004) 203.
65 Y. K. Kwon, A. Boller, M. Pyda and B. Wunderlich, Polymer, 41 (2000) 6237.
66 M. Pyda, J. Polymer Sci., Part B: Polym. Phys., 39 (2001) 3038.
67 M. Pyda, Macromolecules, 35 (2002) 4009.

DOI: 10.1007/s10973-007-8644-0